

# Improving the performance of light-sensitive developer-soluble anti-reflective coatings by using adamantyl terpolymers

Jim D. Meador<sup>a</sup>, Joyce A. Lowes<sup>a</sup>, Charlyn Stroud<sup>a</sup>, Sherilyn Thomas<sup>a</sup>, Yilin Qiu<sup>a</sup>,  
Ramil-Marcelo L. Mercado<sup>a</sup>, Victor Pham<sup>b</sup>, and Mark Slezak<sup>b</sup>

<sup>a</sup>Brewer Science, Inc., 2401 Brewer Drive, Rolla, MO 65401, USA

<sup>b</sup>JSR Micro, Inc., 1280 North Mathilda Avenue, Sunnyvale, CA 94089, USA

## ABSTRACT

In a search for improved resolution and processing latitude for a family of light-sensitive developer-soluble bottom anti-reflective coatings (BARCs), the structure of the binder terpolymer was altered by incorporating acid-cleavable adamantyl methacrylates. Contrast curves and 193-nm microlithography were then used as tools in developing a novel developer-soluble adamantyl BARC which does not include a photoacid generator (PAG) or quencher, but instead depends on acid diffusing from the exposed resist for development. This formulation eliminates concern about PAG or quencher leaching out of the BARC during application of the photoresist. Resolution for a resist A and the new BARC was 150-nm L/S (1:1) for both 38-nm and 54- to 55-nm BARC thicknesses. Resolution and line shape were comparable to that of the non-adamantyl control BARC with same resist at 55-nm BARC thickness, with both BARCs giving some undercutting using an Amphibian™ XIS interferometer for the 193-nm exposures. Light-sensitive adamantyl BARCs that do require inclusion of a PAG for optimum lithography with resist A are also described in this paper. The series of developer-soluble adamantyl BARCs were solution and spin-bowl compatible. The 193-nm optical parameters (n and k) for all adamantyl BARCs were 1.7 and 0.5-0.6, respectively.

**Keywords:** anti-reflective, BARC, light-sensitive, developer-soluble, adamantyl, 193-nm microlithography

## 1. INTRODUCTION

With the IC industry continuing to move to smaller feature sizes to increase information storage capabilities, outstanding anti-reflective techniques will be required to provide the needed critical dimension (CD) control for 193-nm lithography. BARCs will be the anti-reflective materials of choice for critical and even noncritical applications such as implant.<sup>1, 2</sup> A dyed resist with top anti-reflective coating (TARC) will not be sufficient for 45-, 32-, and 22-nm node implant layers. The desired CD for implant for the former node is about 150 nm and for the latter two nodes for implant about 130 nm.<sup>3</sup>

An organic BARC is used under the photoresist to minimize reflectivity from the substrate, improve focus/exposure latitude, reduce both reflective notching and CD swing effects over topography, and potentially protect the 193-nm resist against substrate poisoning.<sup>1, 4</sup> While the BARCs being used for the majority of present-day applications are plasma-developed (dry), the less used developer-soluble (wet) BARCs offer certain advantages including eliminating the reactive ion etching (RIE) step and any damage to plasma-sensitive layers. The exposed resist and developer-soluble BARC are removed in the same step in aqueous tetramethylammonium hydroxide (TMAH). These developer-soluble anti-reflective coatings increase the etch budget by minimizing the removal of non-exposed resist during the BARC development step.<sup>3</sup> Developer-soluble BARCs do not typically provide the resolution achievable with dry BARCs and are aimed at noncritical applications such as implant layers, where resolution requirements are not so severe. The emerging generations of 248- and particularly 193-nm developer-soluble BARCs are usually light-sensitive. Differing from the older generation polyamic acid developer-soluble BARCs, which tend to develop isotropically, these light-sensitive products offer the potential for anisotropic development.<sup>5</sup>

Many different chemical platforms for preparing light-sensitive, positive-working, developer-soluble BARCs have been described in previous papers.<sup>1, 3, 5-10</sup> The best of these are thermosetting and include a) a dye-filled BARC using a polymeric binder,<sup>3, 5</sup> b) an acid-degradable hyperbranched polymer with polymer-bound chromophore,<sup>10</sup> and c) a dye-

attached linear polymer.<sup>1</sup> For these three highlighted approaches, the polymer films become solvent insoluble (crosslinked) during a hot plate bake step. Upon exposure to an appropriate light source and a subsequent post-exposure bake (PEB), they all degrade to developer- or water-soluble materials. This paper deals specifically with the latter platform in which the BARCs are often prepared by combining a linear polymer with chemically attached chromophore and carboxylic acid moieties with 1) a multifunctional crosslinker, 2) PAG, 3) quencher, and 4) solvent. The chemistry for this type of BARC was graphically depicted in an earlier paper.<sup>1</sup> The linear binder polymer for the 193-nm developer-soluble BARCs is usually derived from a monomer with a crosslinkable function, a monomer containing a chromophore, and a monomer with an acid-cleavable group. With the objective being to improve the resolution and processing latitude of developer-soluble BARCs as compared to our earlier generation light-sensitive products, the structure of the BARC's linear terpolymer was varied by changing only the monomer with an acid-labile function. Adamantyl acrylate monomers reportedly provide high contrast after development, as well as transparency at 193 nm.<sup>11</sup> Thus, the standard acid-cleavable alkyl ester in our terpolymerization recipe was replaced with an acid-labile adamantyl methacrylate. Numerous adamantyl methacrylates were included in the study. While the acid-labile constituent usually comprised only a small molar percentage of the binder polymer, this alteration of the terpolymer produced dramatic changes in 1) the derived BARCs' contrast curves and dose-to-clear ( $E_0$ ) and 2) said BARCs' performance in 193-nm lithography. The discussions in this paper include terpolymer and BARC chemistry, BARC film and optical properties, compatibilities, contrast curves, and lithography.

## 2. METHODOLOGY

Solvents for the developer-soluble BARCs included the industry-accepted propylene glycol monomethyl ether (PGME) and propylene glycol monomethyl ether acetate (PGMEA), with the BARCs all end-point filtered prior to testing. The BARC bake was always 160°C for 60 seconds, with the spin application for about 52-56 nm of baked films being 1500 rpm for 30 or 60 seconds. A Gaertner ellipsometer was used to measure film thickness of spin applied, thermoset, stripped, and developed coatings on a silicon substrate. The previously described ethyl lactate (EL) stripping test was used to assess solubility in photoresist solvents.<sup>12</sup> The BARC post-exposure bake (PEB) conditions are given, where needed, for each figure. The effects of 0.26 normal (N) aqueous TMAH developer on both light-exposed and unexposed (dark loss) BARC coatings were measured using a 45-second puddle, a 5-second deionized water rinse, and a spin dry. The optical parameters for the BARCs were measured using a J.A. Woollam Co. Inc. VASE<sup>®</sup> ellipsometer. Weight-average molecular weight ( $M_w$ ) and dispersivity ( $D$ ) were measured using gel permeation chromatography (GPC). Contrast curves for the 193-nm BARCs were prepared using an Oriel<sup>™</sup> DUV broadband exposure unit, with the light passing through a 248-nm bandpass filter prior to the exposures. The 193-nm exposures for lithography using a photoresist were carried out on an Amphibian XIS interferometer from Amphibian Systems. The scanning electron microscope (SEM) photos of cross-sectioned wafers were prepared using a LEO 1560 from Carl Zeiss SMT Incorporated. All of the adamantyl methacrylate monomers that were used in the study came from Idemitsu Kosan Co., Ltd. The 193-nm photoresist used for contrast curves and lithography was identified only as resist A.

## 3. RESULTS AND DISCUSSION

### 3.1 Terpolymer and BARC chemistry

The acid-cleavable adamantyl monomers for this study included 2-isopropyl-2-adamantyl methacrylate (IPM), 2-ethyl-2-adamantyl methacrylate (EM), (2-adamantyloxy)methyl methacrylate (AM), 2-[(2-methyl-adamantyl)oxycarbonyl]methyl methacrylate (MACM), and 2-(cyanomethyl)-2-adamantyl methacrylate (CAM). The structures for these adamantyl monomers are shown in Figure 1. Each adamantyl monomer was terpolymerized with the crosslinkable monomer  $\alpha$ , and the monomer with attached chromophore  $\beta$  using a standard polymerization recipe. The BARCs were prepared by combining the terpolymer with crosslinker, solvent, and usually (at least initially) PAG and quencher. Properties of the derived terpolymer BARCs were then compared with those of the standard (non-adamantyl) alkyl ester terpolymer BARC.

### 3.2 Synthesis and characterization of adamantyl terpolymers

All terpolymers were prepared using identical time/temperature reaction parameters via a free-radical solution polymerization and then purified. The molar ratios for monomer  $\alpha$  and monomer  $\beta$  were constants, when using 12.9 mol percent acid-labile monomer. In one example only, the acid-labile adamantyl monomer's molar percentage

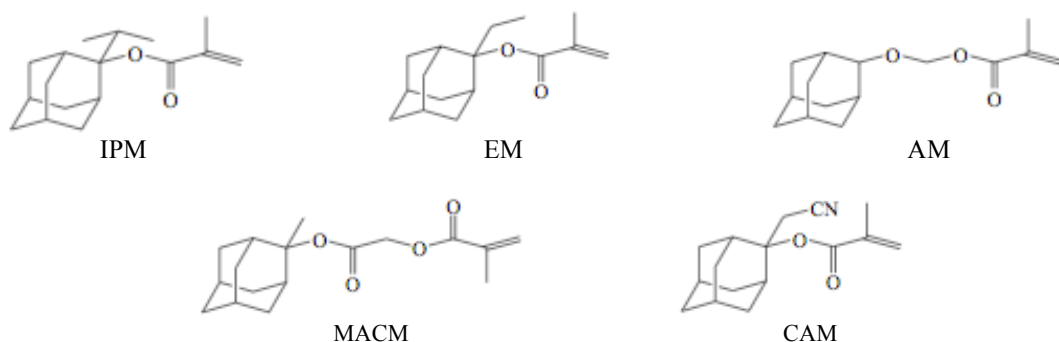


Figure 1. Structures of adamantyl methacrylate monomers.

amongst the three monomers was increased to 21.9 (terpolymer VII), primarily at the expense of crosslinkable monomer  $\alpha$ . The molar percentage of chromophore-bearing monomer  $\beta$  never varied to any extent. The calculated polymer solids, based on charged monomers and initiator, were in all cases near identical. The identity of the terpolymer, identity of the acid-labile monomer, and terpolymer molecular weights are given in Table I. The Mw's for all seven terpolymers were in a moderately narrow range, i.e., 14,950 to 19,600 for purified material.

Table I. Description of terpolymers.

Identity of Terpolymer	Acid-labile Monomer	Terpolymer Molecular Weight (Mw)
I	IPM	16,050
II	EM	16,850
III	AM	19,150
IV	CAM	14,950
V	MACM	17,900
VI	alkyl ester	19,600
VII	EM (21.9 mol%)	15,700

### 3.3 BARC film and optical properties

An identical weight of each of the terpolymers was used in a standard BARC formulation. For all BARC formulations highlighted in Table II, the identities and weights of crosslinker, PAG, quencher, and solvent were constants. After the standard spin and bake, all of the adamantyl BARCs and our standard alkyl ester control showed good resistance to EL and minimal dark loss. A positive number for these two tests signifies swelling. The 193-nm  $n$  and  $k$  values for the terpolymer BARCs were 1.7 and 0.48-0.56, respectively. The film and optical properties data for the BARCs are shown in Table II.

Table II. BARC film and optical properties.

Identity of BARC	Terpolymer	EL Stripping	Dark Loss	193-nm $n/k$
1	I	+0.5%	+0.0%	1.69/0.54
2	II	+1.3%	+0.2%	1.70/0.54
3	III	+0.4%	+0.0%	1.68/0.51
4	IV	+0.4%	+0.3%	1.67/0.51
5	V	+0.8%	+1.8%	1.72/0.48
6	VI	+0.9%	-0.8%	1.68/0.56
7	VII	+0.4%	-1.5%	1.69/0.49

### 3.4 BARC compatibilities

The adamantyl BARCs performed well in compatibility evaluations, i.e., both solution and spin-bowl compatibility (SBC). The reason for solution compatibility testing is to determine whether there will be precipitation in the drains or spin-bowl during mixing of BARC and solvent. About 90 weight % solvent and 10 weight % BARC were mixed at room temperature, followed by mixing 90 weight % BARC and 10 weight % solvent at the same temperature. Any precipitation or fogginess constituted a failure or concern. The testing solvents included PGME, PGMEA, acetone, EL, and  $\gamma$ -butyrolactone/n-butyl acetate (70/30 w/w). BARCs 1, 2, 3, 6, and 7 were solution compatible with a variety of solvents, with the only observed failure (fogginess) being 90/10 by weight acetone/BARC 7. The relatively high EM content in the terpolymer for BARC 7 likely caused this one failure.

SBC testing indicates whether there will be a problem in removing dried BARC from the walls of the spin-bowl by subsequent spin applications of BARC, resist, or solvents. The BARCs were spin-applied to silicon wafers, but not baked. After the coating was dried for 24 hours at ambient conditions, BARC thicknesses were measured (i.e., 51 -56 nm), and a testing solvent was puddled onto the wafer for 3 minutes and then spun off. The wafer was then baked at 100°C for 30 seconds and the BARC thickness re-measured. Removal of less than 90% of the BARC represents a failure. The SBC data for BARCs 1, 2, 3, 6, and 7 may be seen in Figure 2. All BARCs were acceptable for SBC.

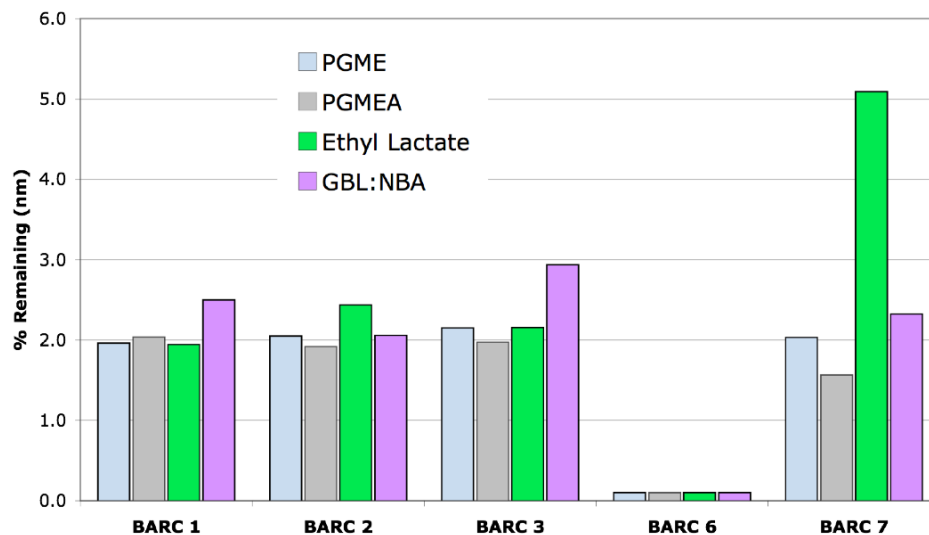


Figure 2. SBC testing results.

### 3.5 Contrast curves

The contrast curves for BARCs 1, 2, 3, 6, and 7 were compared using the Oriel DUV light source with a 248-nm bandpass filter for the exposures. The experimental setup for the exposures was displayed in a previous paper.<sup>3</sup> The BARCs were all baked (thermoset), resulting in film thicknesses of about 53 to 56 nm, and then stripped with EL to simulate the application of a photoresist. A simulated resist PAB was not used for the BARCs, in the absence of a covering resist. The initially selected PEB was at 110°C for 60 seconds. Without a resist, none of the five BARCs cleared in the contrast curve measurements (see Figure 3a). BARC 7 (terpolymer with high EM content) and BARC 1 (IPM terpolymer) came closest to clearing, followed in clearing performance by BARC 2 (terpolymer with low EM content). BARC 3 (AM terpolymer) was comparable to the control, BARC 6.

Using a PEB of 120°C for 60 seconds and again no covering resist or PAB, four of the five same BARCs now cleared in contrast curve studies, with the order of  $E_0$  being BARC 1 < BARC 2 < BARC 3 < BARC 7 < standard alkyl ester terpolymer BARC 6 (see Figure 3b). The control, BARC 6, never cleared.

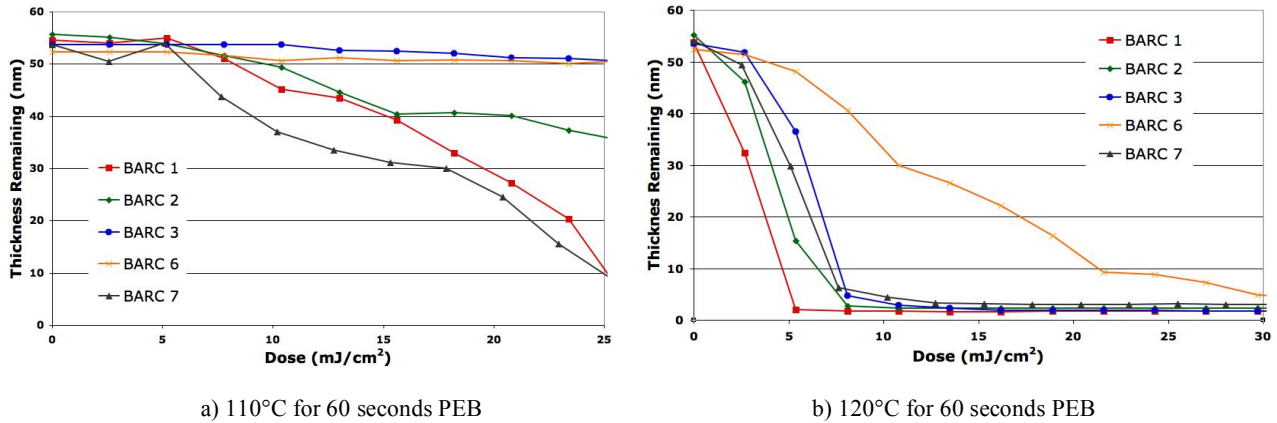


Figure 3. Contrast curves for 193-nm BARCs.

A covering resist A at 195-nm thickness was then applied to same thermoset BARCs at 53- to 56-nm thicknesses. The resist PAB and the PEB were at 110°C for 60 seconds. The contrast curve results were much different than without a resist - with BARCs 1, 2, and 7 clearing (see Figure 4 for order). Photogenerated acid from the photoresist likely contributes to the cleavage of acid-sensitive function in the cured BARC. The change in thickness at  $E_0$  for photoresist A and BARC 1 was close to a vertical drop. BARC 3 and the standard BARC 6 still did not clear at this low PEB. The mediocre  $E_0$  ranking for BARC 3 is surprising considering the literature report of high acid sensitivity for the AM monomer.<sup>11</sup> As will be shown, poor clearance in contrast measurements using the 248-nm bandpass filtered light source does not serve as a reliable predictor of poor lithography when an Amphibian interferometer is used for the 193-nm exposures. Differing sensitivities of PAG in the BARC and photoresist to 248- and 193-nm light might explain this discrepancy.

### 3.6 Lithography for BARCs 1, 2, 3, and 6

Using resist A and an Amphibian interferometer for exposures gave a different order for performance in lithography than might be anticipated from the contrast curve results. The standard alkyl ester platform (BARC 6) was the best in the series of four BARCs giving 150-nm L/S at three different exposure times (1.2, 1.4, and 1.6 seconds), albeit with undercutting. Line collapse occurred for at least one of the three same exposure times for the other three BARCs, with the order of best lithography performance to worst being BARC 3, BARC 2, BARC 1 (see Figure 5). Complete line collapse occurred for all three exposures when using BARC 1 (IPM terpolymer), the product with lowest  $E_0$  with covering resist A. Other photoresists or different light sources will likely give different lithography results for the series of BARCs. A proper mating of photoresist and BARC exposure requirements and development rates is an important

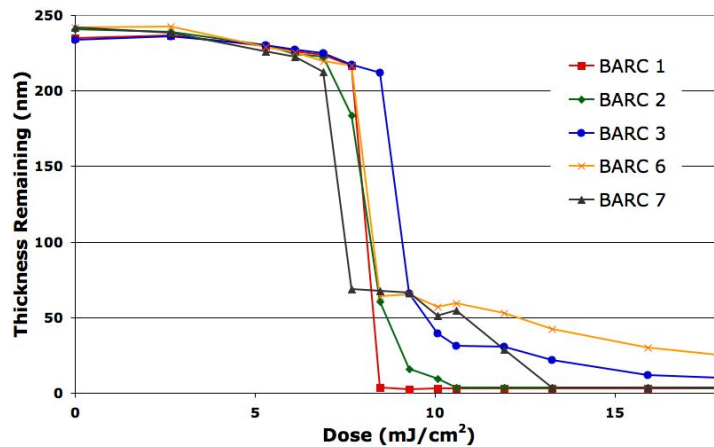


Figure 4. Contrast curves for 193-nm BARCs with covering resist A and a 110°C for 60 seconds PEB.

factor in achieving good lithography, while a vertical drop in the contrast curve for resist on BARC using 248-nm bandpass filtered light is not. Excluding the work shown in Figures 6a, the experimental conditions for all 193-nm lithography described in this paper using the Amphibian interferometer are shown below:

BARC bakes	160°C for 60 seconds
BARC thickness	52-56 nm as measured on silicon after the bake
Thickness of photoresist	195 nm as measured on silicon, after the PAB
PAB for resist on the BARC	110°C for 60 seconds
Exposure times	times are shown near the SEM photos in seconds (sec)
PEB for resist and the BARC	110°C for 60 seconds
Development	0.26N TMAH for 45 seconds

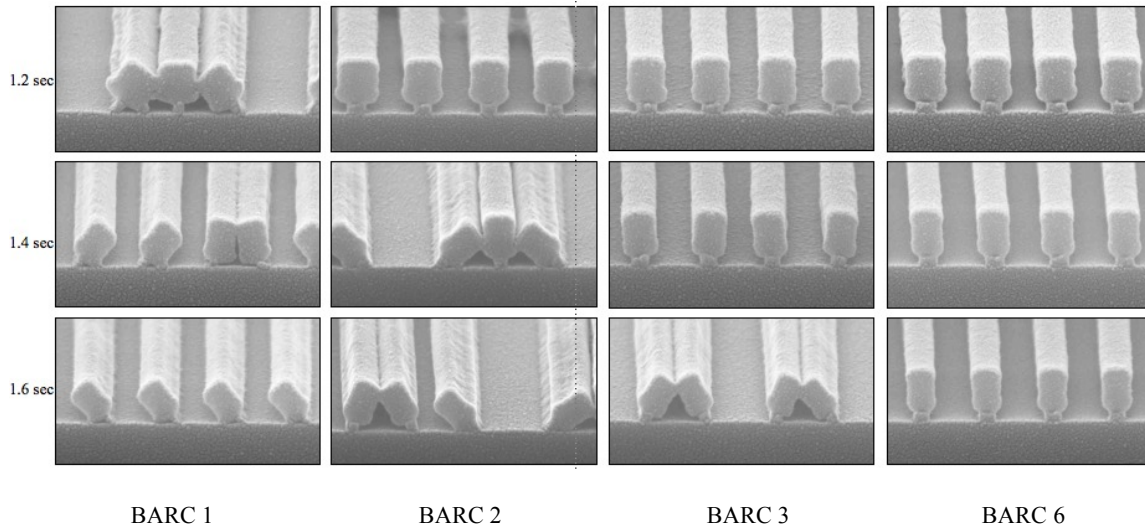
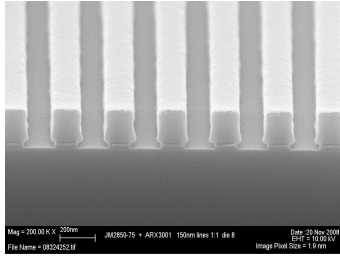


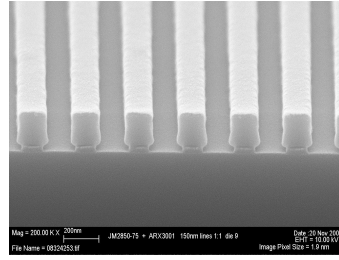
Figure 5. Lithography for BARCs 1, 2, 3, and 6 using resist A and an Amphibian for exposures.

### 3.7 PAG-free and quencher-free derivative of BARC 1

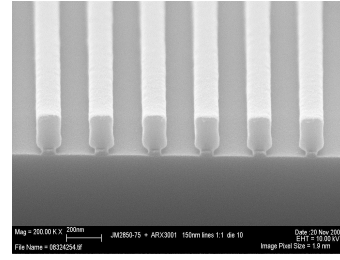
The PAG in the photoresist can contribute to cleaving acid-labile function in the cured BARC by acid diffusion.<sup>13</sup> In response to the low  $E_0$  of BARC 1 with covering resist A and the resist lines collapsing in lithography using resist A, BARC 1 was reformulated by simply leaving out the PAG and quencher and giving BARC 1A. This formulation was spin applied and baked giving a) 38 nm and b) 54-55 nm of cured BARC films. Resist A was applied to the two BARC thicknesses, with all experimental conditions other than the 38-nm BARC thickness continuing to be as described in Subsection 3.6. The SEM data for three different exposure times for both of the BARC thicknesses are shown in Figure 6. Good 150-nm L/S (1:1) were obtained for both BARC thicknesses, although with some undercutting. The BARC film thickness (38 nm versus 54-55 nm) did not significantly affect the L/S patterns. There may be some concern about through-pitch performance, since the undercutting is somewhat dependent on exposure time. A hypothesis was that the line undercutting occurred due to horizontal as well as vertical diffusion of photogenerated acid from the photoresist. However, that may not be the correct or only cause of the observed undercutting.



1.6 seconds

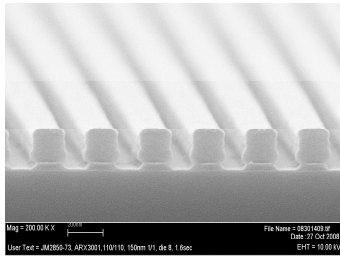


1.8 seconds

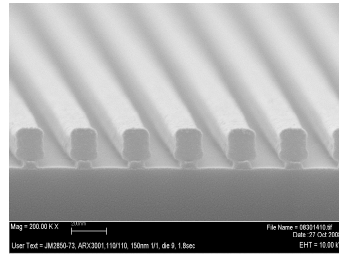


2.0 seconds

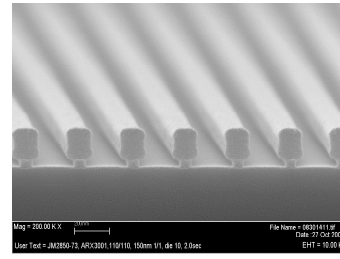
a) 38 nm of BARC 1A



1.6 seconds



1.8 seconds



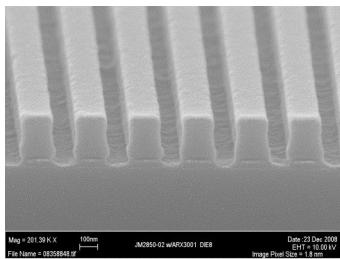
2.0 seconds

b) 54-55 nm of BARC 1A

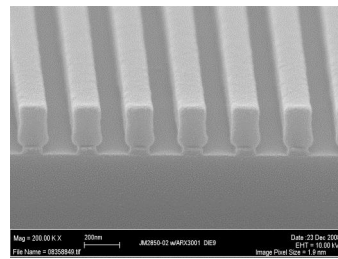
Figure 6. Lithography for resist A on BARC 1A.

### 3.8 PAG-free and quencher-free derivative of BARC 2

The contrast curves shown in Figures 3b and 4 and the lithography shown in Figure 5 indicated that BARC 2 (terpolymer with low EM content) requires slightly more energy for acceptable clearing than BARC 1 (IPM terpolymer). In an attempt to improve on the undercutting observed in lithography with resist A and BARC 1A, BARC 2 was also reformulated by removing PAG and quencher and thus giving BARC 2A. Lithography using resist A on BARC 2A is shown in Figure 7. There was only slight exposure latitude separating scum and undercutting for the best two exposure times shown for this EM BARC. An exposure time of 1.6 seconds produced scum between the lines, while the spaces were clean for an exposure time of 1.8 seconds but the lines were undercut. Defying expectations, resist A on BARC 2A did not provide the desired improvement in line shape when compared to resist A on BARC 1A.



1.6 seconds



1.8 seconds

Figure 7. Lithography for resist A on BARC 2A.

### 3.9 PAG-free and quencher-free derivative of BARC 7

BARC 7 was converted to BARC 7A by removing PAG and quencher from the formulation, as well as half the crosslinker. Lithography using resist A on the BARC and the experimental conditions described in Subsection 3.6 did not provide proper clearance, as shown below in Figure 8. The spaces came close to clearing using the longest exposure time of 2.0 seconds, but the lines were also undercut.

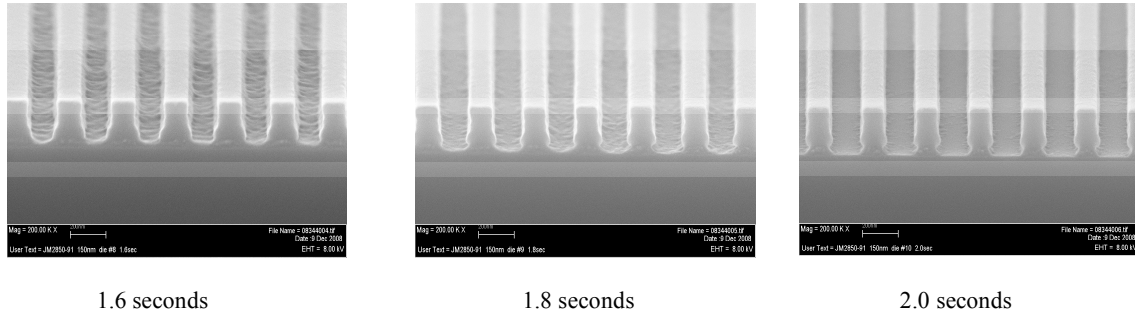


Figure 8. Lithography for resist A on BARC 7A.

### 3.10 Lithography using BARC 4 (CAM terpolymer)

BARC 4 (CAM terpolymer), containing the standard types and quantities of PAG and quencher and described in Table II, did not clear in a 248-nm bandpass filter contrast curve study using covering resist A and a PEB of 110°C for 60 seconds. The lithography with same resist A and the Amphibian tool for exposures, using the processing conditions described in Subsection 3.6, resulted in standing lines but with scum between the lines for all exposure times, therefore a PAG-free and quencher-free formulation was not tested. The observance of poor BARC clearance for both the contrast curve measurements and lithography might result from the electron-withdrawing cyano function destabilizing cleavage of ester and adamantyl function, with the inadequately deprotected terpolymer not sufficiently acidic after the PEB for development. Increasing the PAG content or decreasing quencher loading in the BARC are possibilities for improving cleanliness of the spaces, but the lines are beginning to show undercutting and/or a bulb at their base with 1.8 seconds of exposure, which raises some concerns about hopes for a robust processing latitude. The SEM photos are shown in Figure 9.

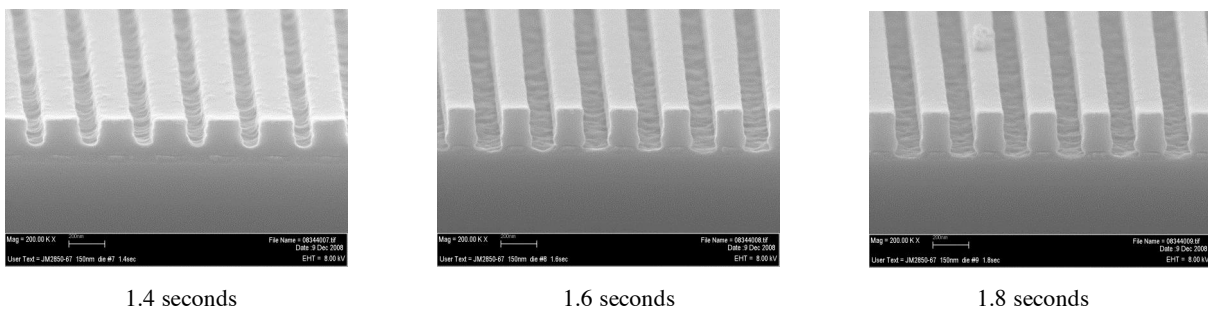


Figure 9. Lithography for resist A on BARC 4.

## CONCLUSIONS

This paper describes our efforts to improve the resolution and processing robustness of a family of 193-nm developer-soluble BARCs by including acid-cleavable adamantyl monomers in the binder terpolymer. Many of the resulting adamantyl BARCs were much more susceptible to acid-deprotection than the standard alkyl ester BARC as shown by contrast curves and lithography. The adamantyl terpolymer BARC providing the best lithographic performance with resist A contained neither PAG nor quencher, instead depending on diffusing acid from the exposed photoresist for development. This BARC yielded similar performance to our standard material, BARC 6. This study requires



additional work that will include exposures with a stepper and through-pitch lithography. The adamantyl BARCs offer good compatibilities and reflectivity control.

## ACKNOWLEDGMENTS

Stephen Gibbons, Hai Xuan, Marc Weimer, Mariya Nagatkina, and Trisha May are members of Brewer Science's Analytical Services Team and are acknowledged for their contributions to this program. John Thompson, Denise Howard, and Eric Stewart are members of same company's SEM Team and provided the very important SEM data.

## REFERENCES

1. Jim Meador, Carol Beaman, Joyce Lowes, Carlton Washburn, Ramil Mercado, Mariya Nagatkina, and Charlyn Stroud, "Development of 193-nm wet BARCs for implant applications," *Proc. SPIE*, 6153, pp. 854-863, 2006.
2. Carlton Washburn, Ramil Mercado, Douglas Guerrero, Jim Meador, "Controlling CD and process window limits for implant patterning," *Solid State Technology*, 49, No. 10, pp. 53-56, 2006.
3. Ramil-Marcelo L. Mercado, Joyce A. Lowes, Carlton A. Washburn, and Douglas J. Guerrero, "A novel approach to developer-soluble anti-reflective coatings for 248-nm lithography," *Proc. SPIE*, 6519, pp. 65192X-1-65192X-10, 2007.
4. Xie Shao, Alice Guerrero, and Yiming Gu, "Wet-Developable Organic Anti-Reflective Coatings for Implant Layer Applications," *SEMICON China 2004 SEMI Technology Symposium*, pp. 1-9, March 17, 2004, [www.brewerscience.com/arc\\_news/arc\\_publications.html](http://www.brewerscience.com/arc_news/arc_publications.html).
5. Jim D. Meador, Carol Beaman, Charlyn Stroud, Joyce A. Lowes, Zhimin Zhu, Douglas J. Guerrero, Ramil-Marcelo L. Mercado, and David Drain, "Dual-layer dye-filled developer-soluble BARCs for 193-nm lithography," *Proc. SPIE*, 6923, pp. 69232W-1-69232W-11, 2008.
6. Douglas J. Guerrero and Tonya Trudgeon, "A new generation of bottom anti-reflective coatings (BARCs): photodefinable BARCs," *Proc. SPIE*, 5039, pp. 129-135, 2003.
7. D.C. Owe-Yang, B-C. Ho, S. Miyazaki, T. Katayama, K. Susukida, W. Kang, and Y.-C. Chang, "Application of photosensitive BARC and KrF resist on implant layers," *Proc. SPIE*, 5376, pp. 452-460, 2004.
8. Francis Houlihan, Alberto Dioses, Medhat Toukhy, Andrew Romano, Joseph Oberlander, HengPeng Wu, Salem Mullen, Alexandra Krawicz, PingHung Lu, and Mark Neisser, "Second Generation Radiation Sensitive Developable Bottom Anti Reflective Coatings (DBARC) and Implant Resists Approaches for 193nm Lithography," *Proc. SPIE*, 6519, pp. 6519OL-1-6519OL-8, 2007.
9. Francis Houlihan, Alberto Dioses, Lin Zhang, Joseph Oberlander, Alexandra Krawicz, Sumathy Vasanthan, Meng Li, Yayi Wei, PingHung Lu, and Mark Neisser, "Second Generation Radiation Sensitive 193 nm Developable Bottom Anti Reflective Coatings (DBARC): Recent Results," *Proc. SPIE*, 6923, pp. 692330-1-692330-7, 2008.
10. Ramil-Marcelo L. Mercado, Hao Xu, Joyce A. Lowes, Jim D. Meador, and Douglas J. Guerrero, "Acid-degradable hyperbranched polymer and its application in bottom anti-reflective coatings," *Proc. SPIE*, 7140, pp. 71402W-1-71402W-11, 2008.
11. Kazuya Fukushima, Shinji Tanaka, Nobuaki Matsumoto, Hidetoshi Ohno, Naoya Kawano, Hideki Yamane, Naoyoshi Hatakeyama, Katsuki Ito, "Leading-edge adamantyl polymers designed for 193 nm lithography," *Proc. SPIE*, 6923, pp. 692335-1-692335-9, 2008.
12. Jim D. Meador, Doug Holmes, William L. DiMenna, Mariya Nagatkina, Michael Rich, Tony D. Flaim, Randy Bennett, and Ichiro Kobayashi, "193-nm Multilayer Imaging Systems," *Proc. SPIE*, 5039, pp. 948-957, 2003.
13. Douglas J. Guerrero, Ramil Mercado, Carlton Washburn, and Jim Meador, "Photochemical Studies on Bottom Anti-Reflective Coatings," *J. Photopolym. Sci. and Technol.*, 19, No. 3, pp. 343-347, 2006.